Hindawi Publishing Corporation
EURASIP Journal on Wireless Communications and Networking
Volume 2008, Article ID 735732, 11 pages
doi:10.1155/2008/735732

Research Article

Intelligent Modified Channel and Frequency Offset Estimation Schemes in Future Generation OFDM-Based Packet Communication Systems

Jaemin Kwak,[1] Sungeon Cho,[2] Kitaeg Lim,[3] Pusik Park,[3] Daekyo Shin,[3] and Jongchan Choi[3]

[1] *Division of Marine Electronics and Communication Engineering, Mokpo National Maritime University, 571, Jukgyo-dong, Mokpo-si, Jeollanam-do 530-729, South Korea*
[2] *Division of Computer & Communications Engineering, Sunchon National University, 315, Maegok-dong, Sunchon-si, Jeollanam-do 540-742, South Korea*
[3] *SoC Research Center, Korea Electronics Technology Institute, 68, Yatap-dong, Bundang-gu, Seongnam-si, Gyeonggi-do 463-816, South Korea*

Correspondence should be addressed to Jaemin Kwak, kjm@mmu.ac.kr

Received 30 January 2008; Accepted 5 June 2008

Recommended by Jong Hyuk Park

The channel estimation and frequency offset estimation scheme for future generation orthogonal frequency division multiplexing (OFDM-) based intelligent packet communication systems are proposed. In the channel estimation scheme, we use additional 8 short training symbols besides 2 long training symbols for intelligently improving estimation performance. In the proposed frequency offset estimation scheme, we allocate intelligently different powers to the short and long training symbols while maintaining average power of overall preamble sequence. The preamble structure considered is based on the preamble specified in standardization group of IEEE802.11a for wireless local area network (WLAN) and IEEE802.11p for intelligent transportation systems (ITSs). From the simulation results, it is shown that the proposed intelligent estimation schemes can achieve better mean squared error (MSE) performance for channel and frequency offset estimation error than the conventional scheme. The proposed schemes can be used in designing for enhancing the performance of OFDM-based future generation intelligent communication network systems.

1. INTRODUCTION

Recently, OFDM has been considered as a promising technique for future generation mobile multimedia communication systems with high-speed transmission and higher bandwidth efficiency [1]. OFDM is now a widely spread communication technology such as IEEE802.11a-based WLAN, and it is an attractive candidate technology for IEEE802.11p wireless access in vehicular environments (WAVE)/dedicated short-range communications (DSRCs) which will be a main feature of future generation intelligent transportation systems.

The IEEE802.11a is a published standard which defines medium access control (MAC) and Physical (PHY) layer protocol for indoor wireless LAN communications. It defines an OFDM-based physical layer to operate in the 5 GHz Unlicensed National Information Infrastructure (UNII) band. The operating channels in IEEE802.11a are specified as 20 MHz wide. The use of 20 MHz operating channel allows for high speeds on each channel up to 54 Mbps. On the other hand, IEEE802.11p is an ongoing task group project for intelligent transportation system physical layer. The scope of IEEE802.11p is to create an amendment of IEEE802.11 to support communication between vehicles and the roadside and between vehicles while operating at high speed for communication range of 1000 meters. The amendment will support communications in the 5 GHz bands; specifically 5.850~5.925 GHz band within North America with the aim to enhance the mobility and safety of all forms of surface transportation, including rail and marine. Amendments to the physical layer and medium access control layer will be limited to those required to support communications under these operating environments within the 5 GHz bands [2].

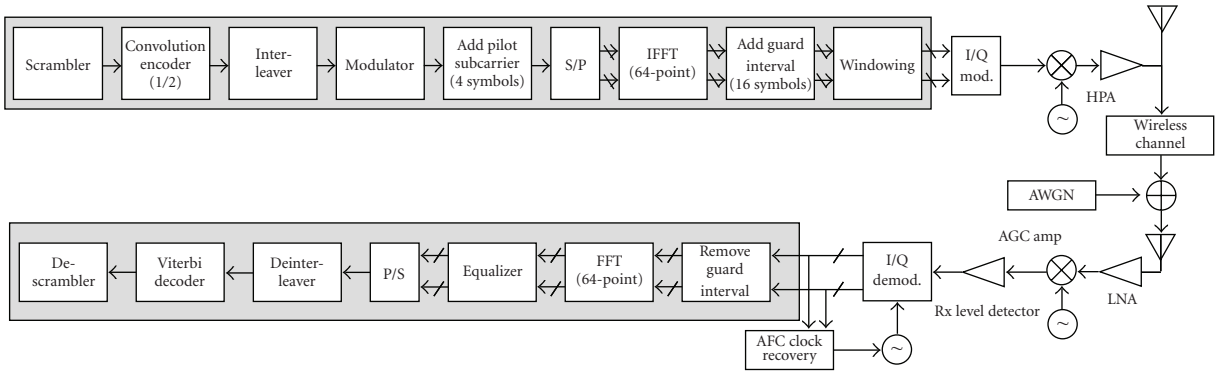

Figure 1: System model of IEEE802.11a and IEEE802.11p physical layers.

In OFDM, the entire channel is divided into many narrow band subchannels, which are transmitted in parallel, thereby, the symbol duration is increased and intersymbol interference (ISI) is reduced. The subcarrier spacing is selected such that modulated carriers are orthogonal over a symbol interval. In addition, a guard interval or cyclic prefix (CP) is inserted to combat the frequency selectivity of the wireless multipath fading channel [3, 4]. In wireless fading channel, since the envelope and phase of signal vary in time and frequency domain, channel estimation process is one of the important components for receiver signal processing. On the other hand, when there is relative motion between the transmitter and receiver, a doppler shift of RF carrier results and introduces a frequency error. Also, there can be residual frequency error caused by frequency instabilities in the oscillators at the transmitter and receiver. In such condition, since the subcarriers of OFDM signal are inherently closely separated compared to the single carrier systems, the tolerable frequency offset becomes very small and frequency offset due to mismatch of the transmitter and receiver carrier frequency is one of the biggest problems [5].

General channel estimation schemes of OFDM-based packet communication systems based on IEEE802.11a or IEEE802.11p mostly use the guided method in the standard document, in which channel estimation algorithm is processed with only two identical long training symbols [3]. As for frequency offset estimation scheme, a frequency offset compensation scheme exploiting entire information of the preamble has been proposed in some papers [6, 7]. In [8, 9], frequency offset estimation schemes using partial preamble information and modified preamble information are proposed for IEEE802.11a systems, respectively.

In this paper, the BER performance of OFDM-based packet communication system is obtained through simulation, and it is shown that the proposed modified channel estimation scheme improves the channel estimation performance of the future generation OFDM-based packet communication systems. At first, the performance of OFDM-based packet communication systems according to frame structure defined in the IEEE802.11a and IEEE802.11p physical layer standards is evaluated in additive white Gaussian noise (AWGN) channel. Then, imperfect channel estimation is considered. After the performance of conventional channel estimation scheme using two identical long training OFDM symbols is evaluated, that with proposed intelligent modified channel estimation scheme using both two long training symbols and additional 8 short training symbols is compared with conventional scheme. The wireless channel used in the channel simulation includes AWGN and frequency selective fading channel implemented by modified HIPERLAN/2 channel model. Also in order to investigate the relationship between performance according to packet length and mobile effect, doppler spread effect is considered. Also, in this paper, an intelligent modified frequency offset estimation scheme is proposed, in which it uses partial short preamble information (3 short training symbols) and full long training symbols with adjustable intelligent long-to-short training symbol power ratio (LSPR).

In the simulation result part, it is shown that the modified channel estimation scheme provides reduced channel estimation error and improves the channel estimation performance due to noise averaging effect maintaining the same preamble format as defined in the IEEE802.11a and IEEE802.11p physical layer specifications. Also it is found that the proposed frequency offset estimation scheme with appropriate intelligent LSPR according to signal-to-noise power ratio (SNR) achieves better frequency offset estimation performance than conventional scheme.

2. OFDM-BASED PACKET COMMUNICATION SYSTEM OVERVIEW

IEEE802.11p physical layer is the special case of IEEE802.11a physical layer standard. That is, the mentioned two physical layer standards have the same system structures and frame formats. However IEEE802.11p uses only 10 MHz frequency bandwidth and the operating frequency band used is 5.850~5.925 GHz.

Figure 1 shows the block diagram of IEEE802.11a and IEEE802.11p system model. In the transmitter part, input data are scrambled to prevent a long sequence of ones or zeros, so that timing recovery at the receiver can be done with easiness. Then the output of the scrambler is encoded by convolutional code and interleaved to prevent

Table 1: System parameters according to data rate.

Data rates [Mbps]		Modulation scheme	Code rate	Coded bits per subcarrier	Data bits per OFDM symbol
IEEE802.11a	IEEE802.11p				
6	3	BPSK	1/2	1	24
9	4.5	BPSK	3/4	1	36
12	6	QPSK	1/2	2	48
18	9	QPSK	3/4	2	72
24	12	16QAM	1/2	4	96
36	18	16QAM	3/4	5	144
48	24	64QAM	2/3	6	192
54	27	64QAM	3/4	6	216

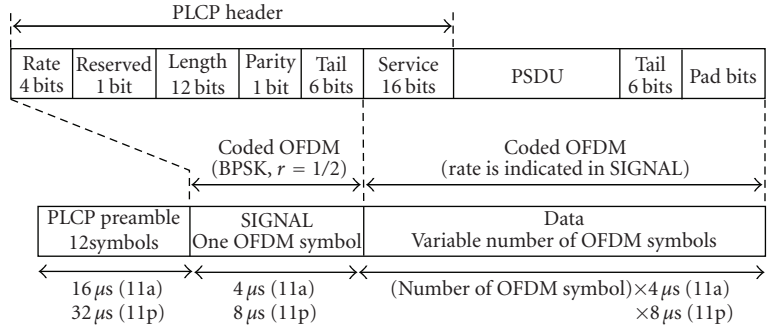

Figure 2: PPDU frame format of IEEE802.11a and IEEE802.11p.

burst error. The interleaved coded bits are grouped and form modulation symbols such as binary phase-shift keying (BPSK), quadrature phase-shift keying (QPSK), and quadrature amplitude modulation (16QAM), 64QAM. After the 48 modulation symbols and 4 pilot symbols are inserted to 64 point inverse fast Fourier transform (IFFT) for making subcarrier modulated OFDM symbols, cyclic prefix (guard interval) is added. In the IFFT input part, remaining 12 subcarriers are not used, and 4 pilot symbols are used for residual phase error estimation at the receiver. At last, cyclic prefix inserted OFDM signal is windowed and transmitted by RF part. At the receiver part with channel experienced received signal, inverse operation of transmitter is done in reverse order.

IEEE802.11a physical layer defines data rates of 6, 9, 12, 18, 24, 36, 48, and 54 Mbps while IEEE802.11p physical layer defines just half rate of that. Table 1 shows the system parameters of IEEE802.11a and IEEE802.11p according to data rates. For mandatory rate mode, code rate of convolutional code is set to only 1/2.

Figure 2 shows frame format which consists of OFDM physical layer convergence protocol (PLCP) preamble, PLCP header, PLCP service data unit (PSDU), Tail bits, and Pad bits. In the PLCP header, RATE, Reserved, LENGTH, Parity, Tail bits are SIGNAL field of one OFDM symbol, which is transmitted only in rate 1/2 coded BPSK modulation for higher communication performance. SERVICE, PSDU, Tail, Pad bits are defined as DATA which is transmitted according to data rate indicated by RATE of header.

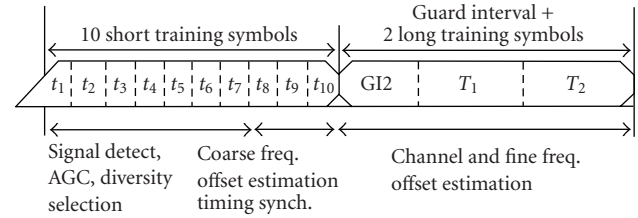

Figure 3: Preamble structure of IEEE802.11a and IEEE802.11p standardization groups.

In the PLCP preamble field shown in Figure 3, we can see preamble consists of 10 identical short training symbols and 2 identical long training symbols. Standard document recommend that short training symbols are used for signal detect, AGC, diversity selection, coarse frequency offset estimation, timing synchronization, and long training symbols are used for channel estimation and fine frequency offset estimation.

3. CHANNEL MODEL

The channel model used in this paper is the frequency-selective fading model. For performance evaluation, we modified delay profile of HIPERLAN/2 channel simulation model D. The HIPERLAN/2 channel model is tapped delay line type of channel model which is basically described in [10]. Original model D describes LOS conditions in a large

Table 2: Modified HIPERLAN/2 model D profile.

Tap number	Delay (ns)	Average relative power (dB)	Ricean factor	Doppler spectrum
1	0	0.0	10	Class+spike
2	100	−1.55	0	Class
3	200	−3.54	0	Class
4	300	−7.03	0	Class
5	400	−8.98	0	Class
6	500	−14.29	0	Class
7	600	−15.80	0	Class
8	700	−inf	0	Class
9	800	−19.59	0	Class
10	900	−22.68	0	Class
11	1000	−inf	0	Class
12	1100	−27.70	0	Class

open space indoor or outdoor environment and its root mean square (RMS) delay spread is about 140 nanoseconds. Modified model D profile with 12 taps is shown in Table 2. The Doppler spectrum in the model consists of classical u-shape and spike shape.

In the table, first tap is Rician fading path and the other taps are Rayleigh fading paths. We used filtered white Gaussian noise (FWGN) model to generate each tap fading samples as shown in Figure 4. The FWGN model is a classical fading generation method, in which WGN samples are filtered by Doppler shaping filter. In this paper, Doppler filter is designed by finite impulse response (FIR) filtering type.

In the channel model, the fading samples of lth tap path in discrete time is described by

$$h_l(n) = \overline{h}_l(n)e^{j2\pi f_d \cdot t_f \cdot n}, \tag{1}$$

where f_d is doppler frequency, t_f is sampling time interval, and $\overline{h}_l(n) = h_I(n) + jh_Q(n)$ is fading channel samples with zero centered Doppler power spectral density (PSD). The real and imaginary part of fading samples are uncorrelated each other as below

$$E\left[h_I(n)h_Q^*(n)\right] = 0. \tag{2}$$

The classical u-shaped Doppler PSD with uniform power azimuth spectrum (PAS) is defined as [11–13]

$$S(f) = \frac{a}{\sqrt{1-\left(f/f_m\right)^2}}, \quad |f| \le f_m, \tag{3}$$

where a and f_m are fading power parameter and maximum Doppler shift, respectively.

Figure 5 shows Doppler power spectrum in which $S(f)$ has infinitive values at $f = \pm f_m$. In this paper we truncated the normalized Doppler frequency region for this spectrum to ± 0.999 to avoid the singularities and to approximate the classical spectrum shape.

Assuming Doppler filter is implemented by FIR-type and filter coefficient is $v_l(m)$, $\overline{h}_l(n)$ is expressed by

$$\begin{aligned}\overline{h}_l(n) &= h_I(n) + jh_Q(n) \\ &= \sum_{m=0}^{M-1} v_l(n)w_I(n-m) + j\sum_{m=0}^{M-1} v_l(n)w_Q(n-m),\end{aligned} \tag{4}$$

where $w_I(n)$ and $w_Q(n)$ are white Gaussian random variables with zero mean and unit variance. As shown in Figure 4(a), Rayleigh fading generator can be constructed by (3), (4).

On the other hand, Rician fading generator is shown in Figure 4(b) which is implemented by adopting additional line-of-sight (LOS) component to Rayleigh fading generator output. In this case, Rician fading samples are obtained by

$$\begin{aligned}\widehat{h}_l(n) &= \sqrt{P_{l,s}}h_l(n) + \sqrt{P_{l,\mathrm{LOS}}}h_l^{\mathrm{LOS}}(n) \\ &= \sqrt{P_{l,s}}\overline{h}_l(n)e^{j2\pi f_d \cdot t_f \cdot n} + \sqrt{P_{l,\mathrm{LOS}}}e^{j2\pi f_{\mathrm{LOS}} \cdot t_f \cdot n},\end{aligned} \tag{5}$$

where $P_{l,s}$ and $P_{l,\mathrm{LOS}}$ are power of scatter (Rayleigh) component and LOS component for lth tap path, respectively. Each power value of the two parameters can be computed using Rician factor, which is defined as LOS component to scatter component power ratio, and total power of lth tap path.

4. PROPOSED INTELLIGENT CHANNEL AND FREQUENCY OFFSET ESTIMATION SCHEMES

The channel estimation is an important task for estimating the frequency response of the radio channel the transmitted signal travels before reaching the receiver front end. On the other hand, frequency offset estimation is also a critical problem in OFDM-based packet communication systems, since OFDM signal is more sensitive to frequency offset compared to single carrier system. In this chapter we describe the preamble of IEEE802.11a or IEEE802.11p physical layer more specifically, and introduce the proposed channel estimation and frequency offset estimation schemes.

As mentioned in this paper, the OFDM preamble is effectively used for channel estimation and frequency offset estimation.

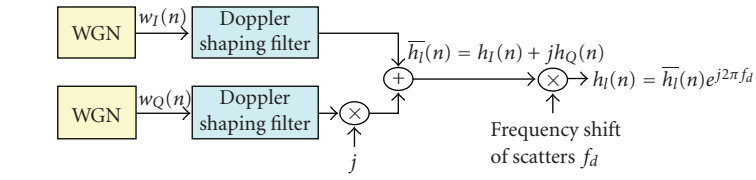

(a) Rayleigh fading generator

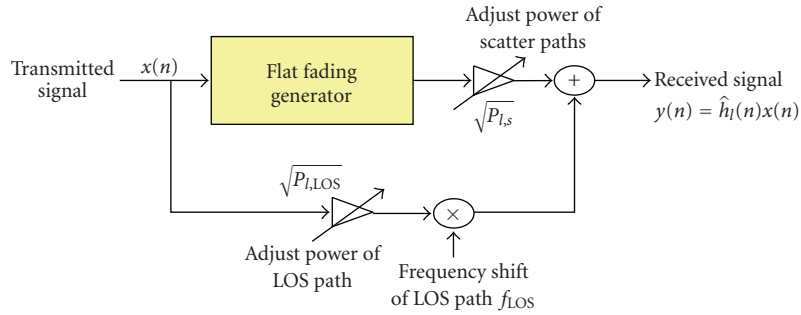

(b) Rician fading generator

Figure 4: Rayleigh and Rician fading generators.

A Short training symbol consists of 12 subcarriers, so training sequence in frequency is defined as

$$S_{-26,26} = \sqrt{\frac{13}{6}} \times \{0,0,1+j,0,0,0,-1-j,0,0,0,1 + j,0,0,0,-1-j,0,0,0,-1-j,0,0,0,1 + j,0,0,0,0,0,0,0,-1-j,0,0,0,-1, - j,0,0,0,1+j,0,0,0,1+j,0,0,0,1 + j,0,0,0,1+j,0,0\}, \tag{6}$$

where multiplication factor of $\sqrt{13/6}$ is power normalization factor.

A long training symbol consists of 53 subcarriers including zero value at dc, so long training sequence in frequency is defined as

$$L_{-26,26} = \{1,1,-1,-1,1,1,-1,1,-1,1,1,1,1,1,1, - 1,-1,1,1,-1,1,-1,1,1,1,1,0,1, - 1,-1,1,1,-1,1,-1,1,-1,-1, - 1,-1,-1,1,1,-1,-1,1,-1,1, - 1,1,1,1,1\}. \tag{7}$$

Short training and long training symbols in time are obtained by IFFT operation of the frequency domain sequences of that. The time sequence of total preamble sequence power in time is shown in Figure 6.

As mentioned earlier, PLCP includes 10 identical short training symbols and two long training symbols that are shown in Figure 6. Each short training symbol consists of 16 samples while long training symbol consists of 64 samples. The 32 samples of GI2 inserted between short and long training symbols are CP of long training symbols. Those properties described above are used for channel estimation and frequency offset estimation scheme.

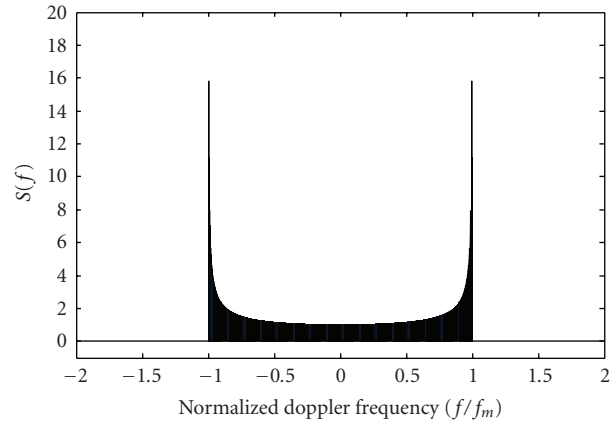

Figure 5: Doppler power spectrum according to normalized doppler frequency.

4.1. Channel estimation scheme

Widely used channel estimation scheme in OFDM-based packet communication such as IEEE802.11a and IEEE802.11p is a method to use known preamble with several specific patterned symbols at the receiver.

The received nth sample of OFDM signal in discrete time domain, y_n, and its FFT output Y_i are expressed by

$$y_n = x_n \otimes h_n + w_n, \qquad Y_i = X_i \times H_i + W_i, \tag{8}$$

where, x_n, h_n, w_n are nth time domain sample of transmitted singal, channel impulse response, and noise component,

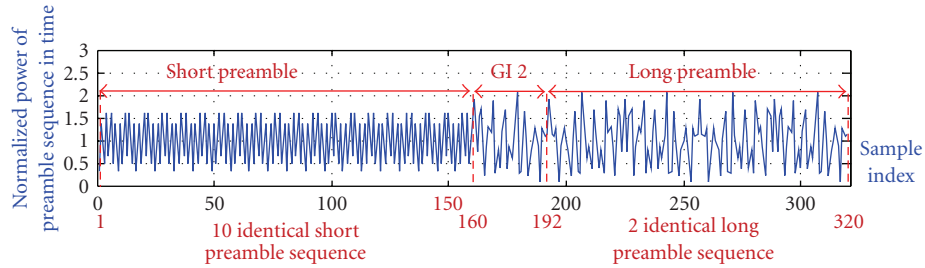

Figure 6: Normalized power signal of IEEE802.11a and IEEE802.11p preamble in time.

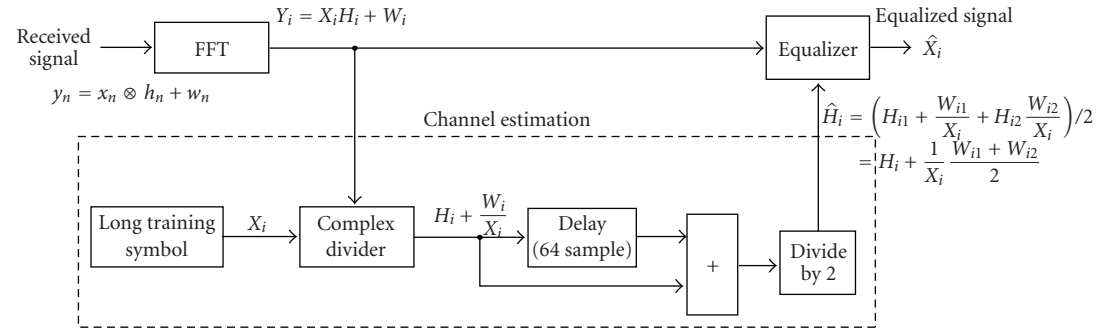

(a) Conventional scheme

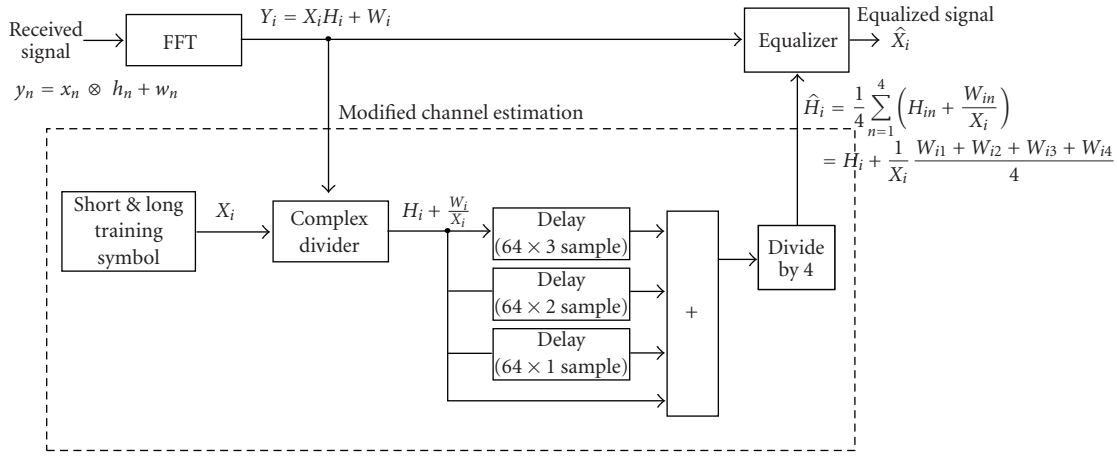

(b) Proposed scheme

Figure 7: Conventional and proposed channel estimation scheme.

respectively. Similarly, X_i, H_i, W_i are corresponding frequency domain samples.

Figure 7 shows the structure of conventional and proposed channel estimation schemes. In conventional channel estimation scheme shown at Figure 7(a), by using two long training sequences, 64×2 values (128 sample values) are used for channel frequency response estimation. By dividing FFT output Y_i by long training symbol, following expression can be obtained:

$$\frac{Y_i}{X_i} = \frac{X_iH_i + W_i}{X_i} = H_i + \frac{W_i}{X}. \tag{9}$$

As expressed in (10), final channel estimation coefficients are obtained [3]:

$$\hat{H}_i = \left(H_{i1} \times \frac{W_{i1}}{X_i} + H_{i2} + \frac{W_{i2}}{X_i}\right) \Big/ 2 \approx H_i + \frac{1}{X_i}\left(\frac{W_{i1} + W_{i2}}{2}\right), \tag{10}$$

where it is assumed that H_{i1} and H_{i2} are almost the same, and H_{in} and W_{in} are ith frequency domain sample values of channel and Gaussian noise for nth long training OFDM symbol.

Figure 7(b) shows proposed modified channel estimation scheme adopted in this paper. In the proposed scheme, both

two long training symbols and 8 short training symbols (last 128 samples) are used for channel estimation. That is, additionally last 128 samples in the short training symbol are used for improving channel estimation capability. Since total 64×4 training sequences are averaged, noise component in the channel estimation values are reduced. However, the enhancement of channel estimation from this scheme is available for only 12 subcarriers position described in (6).

Finally, channel estimation coefficients from the modified scheme is expressed as

$$\hat{H}_i = \frac{1}{4}\sum_{n=1}^{4}\left(H_{in} + \frac{W_{in}}{X_i}\right) \approx H_i \times \frac{1}{X_i}\left(\frac{W_{i1} + W_{i2} + W_{i3} + W_{i4}}{4}\right). \tag{11}$$

4.2. Frequency offset estimation scheme

The IEEE802.11a and IEEE802.11p standardization groups give guidelines on how to use the various segments of the preamble to perform the necessary synchronization function as shown in previous Figure 3 [14–16].

In the preamble structure, parts from t_1 to t_{10} are short training symbols that are all identical and each symbol is 16 samples long, and parts from T_1 to T_2 are long training symbols that are identical and each is 64 samples long. Inserted part of GI2 between short and long training symbols is cyclic prefix of T_2 including 32 samples.

Let $x(n) = x_S(n)$, for $n = 1, 2, \ldots, 160$, and let $x(n) = x_L(n)$, for $n = 161, 162, \ldots, 320$, where $x_S(n)$ denotes sample sequence for short training symbol, and $x_L(n)$ denotes sample sequence for GI2 and long training symbol in time domain at the transmitter. In the proposed scheme, we adopt LSPR parameter of ρ as the long training symbol to short training symbols power ratio for power ratio control parameter between the short and long training symbols. Note that it can be seen that the conventional scheme is an special case ($\rho = 1$) of the proposed scheme. Then, power normalized transmitter signal representation for the short and long training symbols are as follows:

$$s(n) = \begin{cases} \dfrac{1}{\sqrt{P_0}} x_S(n), & n = 1, 2, \ldots, 160 \\ \sqrt{\dfrac{\rho}{P_0}}\, x_L(n), & n = 161, 162, \ldots, 320, \end{cases} \tag{12}$$

where overall average power of original preamble, P_0 , is

$$\begin{aligned} P_0 &= \frac{\sum_{n=1}^{320} \left| x(n) \right|^2}{320} \\ &= \frac{\sum_{n=1}^{160} \left| x_S(n) \right|^2 + \rho \sum_{n=161}^{320} \left| x_L(n) \right|^2}{320}. \end{aligned} \tag{13}$$

In Figure 8, normalized power signal of overall preamble sequence in time is shown according to LSPR parameter. As LSPR value becomes higher, power magnitude of the long preamble (training symbols) becomes larger relative to that of short preamble (training symbols).

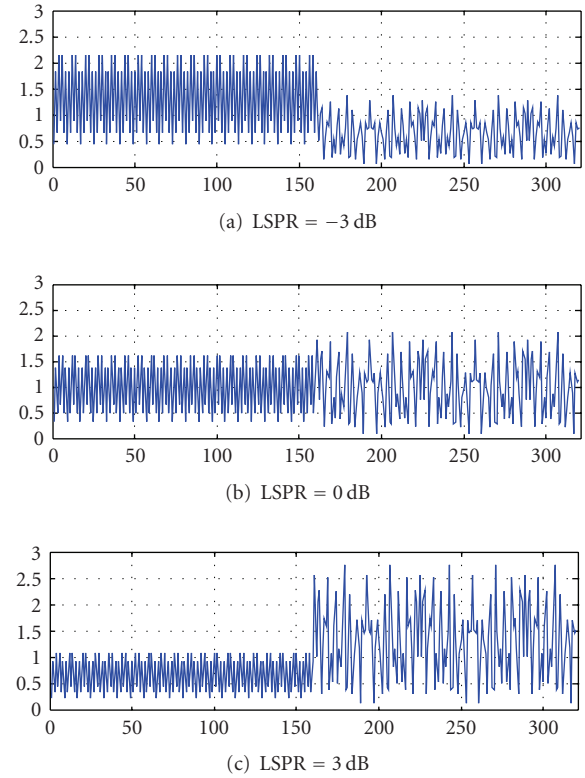

Figure 8: Normalized power sequence of preamble according to LSPR.

As presented in Chapter 2, we assume that signal detection and automatic gain control (AGC) are completed prior to 8th short training symbol start point. So three identical short training symbols (t_8, t_9, t_{10}) and two long training symbols (T_1, T_2) can be used for frequency offset estimation.

The received signal affected by multipath channel, frequency offset, and additive white Gaussian noise after AGC and signal detection can be expressed by

$$r(n) = \sum_{l=1}^{N_h} h_l s(n-l) e^{j2\pi\varepsilon n/N} + v(n), \tag{14}$$

where h_l and N_h are the impulse response and length of multipath channel, respectively, $v(n)$ indicates AWGN samples, N is IFFT/FFT size, and ε is the frequency offset normalized with subcarrier spacing.

As shown in the previous figures, the preamble structure suggests two-stage frequency offset estimation, in which coarse frequency offset estimation and fine frequency offset estimation are performed by the short training symbol and long training symbols, respectively. This two-stage estimation is processed by first acquiring a coarse estimate of the frequency offset from the short training symbol, and then correcting the long training symbols with this estimate [3].

Normalized frequency offset estimation by the short training symbols (t_8, t_9, t_{10}) can be estimated by

$$\hat{\varepsilon}_{sh} = \frac{N}{2\pi \times 16} \times \frac{\left[\arg\left(\sum_{n=113}^{128} r^*(n)r(n+16)\right) + \arg\left(\sum_{n=129}^{144} r^*(n)r(n+16)\right)\right]}{2}. \quad (15)$$

Similarly, normalized frequency offset by the long training symbols (T_1, T_2) can be estimated by

$$\hat{\varepsilon}_{lo} = \frac{1}{2\pi}\left[\arg\left(\sum_{n=193}^{256} r^*(n)r(n+64)\right)\right]. \quad (16)$$

Finally, the overall normalized frequency offset estimation is given as $\hat{\varepsilon} = \hat{\varepsilon}_{sh} + \hat{\varepsilon}_{lo}$.

Because arctangent operation is limited to $[-\pi, \pi]$, frequency offset estimation range is limited as shown in the following [8]:

$$-\pi < \frac{2\pi\varepsilon N_D}{N} < \pi, \quad (17)$$

where N_D is the amount of delay which is 16 and 64 for estimation from the short training and long training symbols, respectively.

Therefore, the frequency offset estimation by (15) and (16) can achieve estimation range of $|\varepsilon| < 2$ and $|\varepsilon| < 0.5$, respectively. Because normalized frequency offset estimation accuracy from the short training symbols only should be better than ± 0.5, to achieve low MSE, we can intuitively prospect that relatively low power is needed for the short training symbols compared to the long training symbols at higher SNR condition, and vice versa at lower SNR.

5. SIMULATION RESULTS

Before simulation of the channel and frequency offset estimation, we obtained system BER performance in AWGN channel environment. In this simulation, soft decision decoded Viterbi algorithm is used for forward error correction (FEC) decoder.

In the Figure 9, we can see that the performance of BPSK and QPSK modes with the same code rate shows the same performance. This performance simulation results can be used for analysis of IEEE802.11a and IEEE802.11p since they have the same system and frame structure. Specifically, at reference BER performance of 10^{-5}, mandatory modes BPSK (QPSK), 16QAM with code rate 1/2, required 4.15 dB and 6.85 dB, respectively.

5.1. Results for channel estimation scheme

Simulation parameters used are given in Table 3. These simulation parameters are suggested based on IEEE802.11p physical layer, however it can be considered for IEEE802.11a physical layer by scaling timing-related parameters properly.

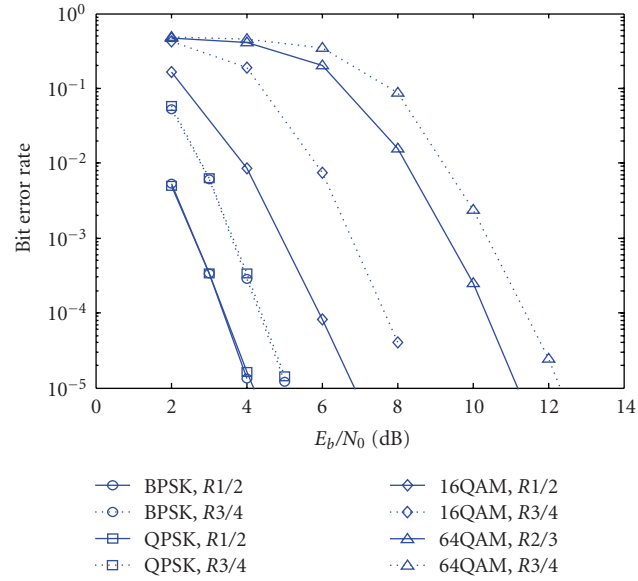

Figure 9: BER performance of IEEE802.11a and IEEE802.11p physical layers in AWGN channel environments.

Table 3: Simulation parameters for channel estimation performance.

Simulation parameter	Value
Modulation/data rate	QPSK/6 Mbps
Constraint length	7
Trellis depth	34
Vehicular speed	30 Km/h, 100 Km/h
Rms delay spread	242 ns
Center frequency	5.9 GHz
SNR	20 dB
Data length per frame	50∼400 bytes

System bandwidth of IEEE802.11p OFDM-based packet communication systems is 10 MHz (20 MHz in case of IEEE802.11a). The subcarrier spacing is 10 MHz/64 = 156.25 KHz (312.5 KHz in case of IEEE802.11a). For mobile application, modified HIPERLAN/2 channel is adopted and vehicle velocities 30 Km/h and 100 Km/h are assumed. In the channel, maximum delay and RMS delay are about 1100 nanoseconds and 242 nanoseconds, respectively.

Figure 10 shows the power magnitude spectrum of IEEE802.11p OFDM-based signal. From the figure we can identify frequency selectivity of the simulated channel, four pilot tone signals which are scaled for identification, and system bandwidth of 10 MHz.

Figure 11 shows BER performance of the system with proposed channel estimation scheme according to packet length under vehicular environment. When we set target BER to be 10^{-3}, packet length must be less than approximately 200 Bytes and 50 Bytes at vehicle speeds 30 Km/h and 100 Km/h, respectively.

Figure 12 shows simulation results for MSE performance under the modified HIPERLAN/2 model D channel

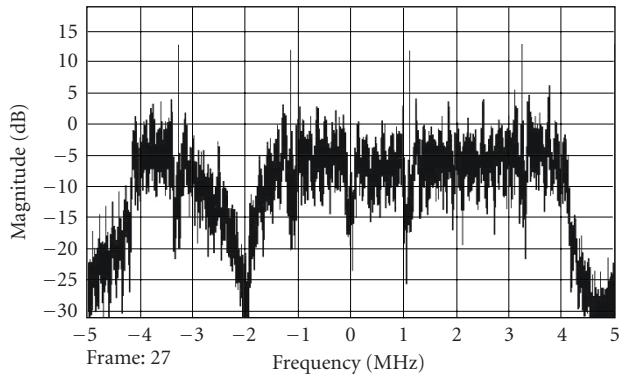

Figure 10: Power spectrum characteristics of the OFDM signal under the frequency-selective fading channel (Eb/No = 10 dB).

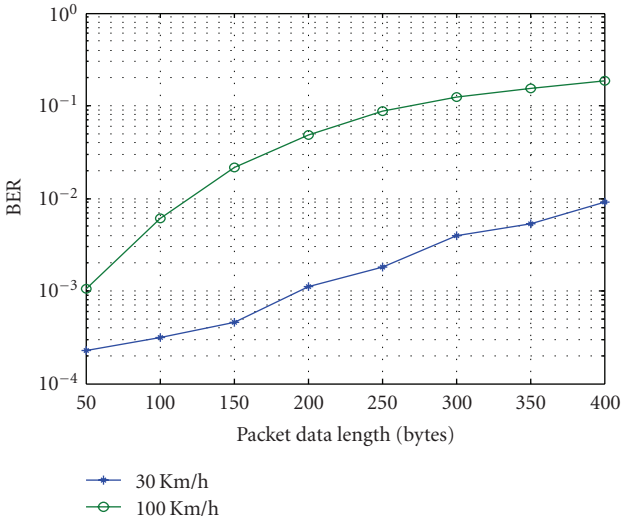

Figure 11: BER performance according to packet length (Eb/No = 10 dB).

according to Eb/No. For each Eb/No values, 100 packets are used for channel estimation error extraction. In the simulation, we only considered channel estimation values for 12 subcarrier indexes because there is only 12 valid subcarriers in which short training values practically exist. When the same MSE is referenced, about 5 dB Eb/No gain could be achieved.

5.2. Results for frequency offset estimation scheme

We have evaluated and compared the performance of the proposed algorithm with conventional one in the HIPERLAN/2 modified frequency selective fading channel. In the simulation, it is assumed that AGC and packet detection is completed, and packet timing is perfectly synchronized. Impulse response of the multipath channel h_l is set to channel model described in chapter 3. Because IEEE802.11a standard specifies a maximum oscillator frequency error of 20 ppm at the transmitter and receiver, assuming carrier center frequency to be 5.805 GHz, normalized frequency

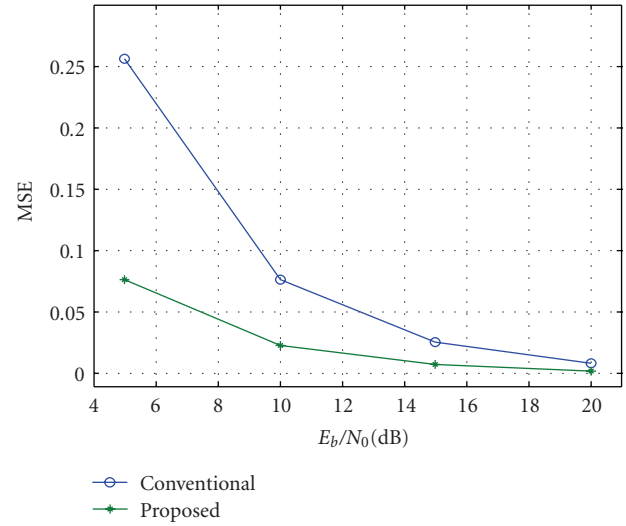

Figure 12: MSE performance comparison between conventional and proposed channel estimation for valid 12 subcarriers.

offset of ε is set to worst case value of 0.74. Also relatively lower value of frequency offset, $\varepsilon = 0.246$, is considered for simulation.

The MSE of the normalized frequency offset estimation error is obtained from 10000 Monte Carlo simulation as a function of SNR.

Figure 13 shows MSE performance of the proposed frequency offset estimation scheme as a function of SNR at $\varepsilon = 0.246$. As previously mentioned, LSPR = 0 dB is the case of conventional frequency offset estimation scheme. From Figure 12, we can observe that conventional scheme shows lower MSE only in the SNR region from −0.42 dB to 1.8 dB, approximately. At other SNR region, proposed scheme with some LSPR values shows lower MSE values according to SNR. If we can assume received SNR is known at the transmitter, we can achieve lowest MSE for the frequency offset estimation error by selecting adequate LSPR value from the proposed scheme. Some SNR estimation scheme is needed to effectively obtain desirable performance.

Figure 14 shows MSE performance curve of the proposed frequency offset estimation scheme as a function of SNR at $\varepsilon = 0.74$. Similar results to Figure 13 are obtained, but the estimation performance is slightly degraded due to more severe condition of frequency offset. In these results, MSE performance shows the lowest value in the region from SNR = −0.4 dB to SNR = 1.88 dB

Table 4 shows relation between SNR condition and corresponding optimized LSPR parameter for $\varepsilon = 0.74$ and $\varepsilon = 0.246$. In the simulation, LSPR parameter value is varied from −6 dB to +9 dB with 3 dB step.

Figure 15 is MSE performance curve according to LSPR parameters obtained through simulation when $\varepsilon = 0.74$ and $\varepsilon = 0.246$. From the simulation results, it is known that MSE performance with proposed estimation scheme is not changed significantly although normalized frequency offset

Table 4: Relation of SNR region condition and corresponding optimized LSPR parameters ($\varepsilon = 0.74$, $\varepsilon = 0.246$).

	SNR region ($\varepsilon = 0.74$)	SNR region ($\varepsilon = 0.246$)
LSPR = −6 dB	< −3.25 dB	< −3.37 dB
LSPR = −3 dB	−3.25∼ − 0.4 dB	−3.37∼ − 0.42 dB
LSPR = 0 dB	−0.4∼1.88 dB	−0.42∼ + 1.8 dB
LSPR = +3 dB	1.88∼5.85 dB	+1.8∼ + 5.7 dB
LSPR = +6 dB	5.85∼7.7 dB	+5.7∼ + 7.56 dB
LSPR = +9 dB	> 7.7 dB	> +7.65 dB

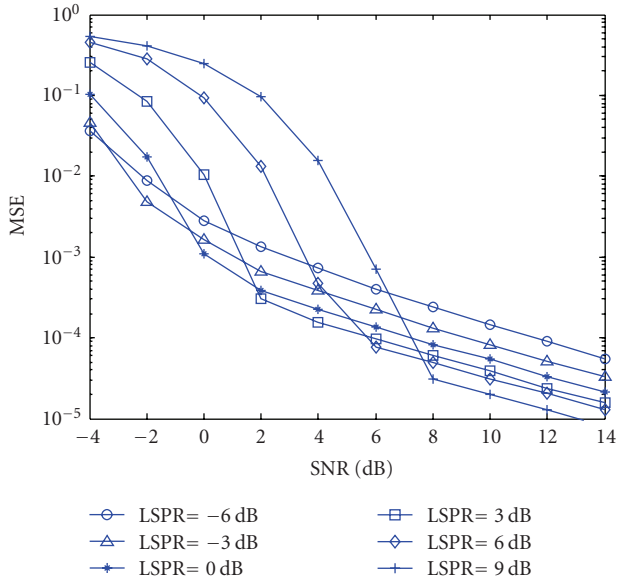

Figure 13: MSE performance of the proposed scheme ($\varepsilon = 0.246$).

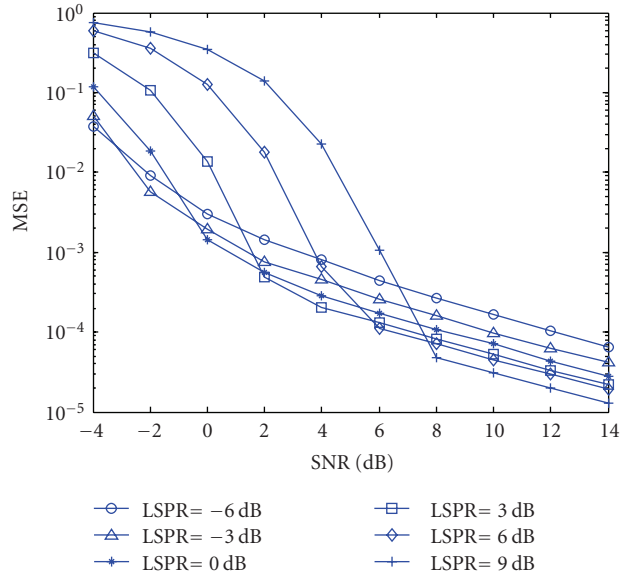

Figure 14: MSE performance of the proposed scheme ($\varepsilon = 0.74$).

error is small or large value. Also there exists an optimum LSPR value according to SNR conditions.

Therefore, we can obtain LSPR parameter value from the figure to achieve better MSE performance according to SNR condition.

If channel state is slowly varying relative to OFDM packet length and SNR estimation value at receiver is transmitted to transmitter, the packet-based communication system with proposed frequency offset estimation scheme can obtain the optimized LSPR parameters at all SNR condition.

Also it is known that the achievable MSE performance curve can be approximated by combining lines with lowest MSE value at each SNR. Therefore proposed scheme can achieve superior frequency offset estimation performance to conventional one by cooperating with appropriate SNR estimation scheme.

6. CONCLUSION

In this paper, some important intelligent estimation techniques in OFDM-based communication system, which is suitable for future generation wireless mobile communication network service, is proposed. Also we have evaluated the estimation performance of an intelligent channel estimation scheme and frequency offset estimation scheme for existing OFDM-based wireless packet communication system such as IEEE802.11a and future generation OFDM-based wireless packet communication IEEE802.11p physical layer.

From the simulation results for conventional and proposed channel estimation scheme, attainable packet length according to Doppler shift is obtained. Also, it is shown that the modified channel estimation scheme provides reduced channel estimation error and improves the channel estimation performance due to noise averaging effect while maintaining the same preamble format as defined in the IEEE802.11a and IEEE802.11p physical layer specifications.

For enhancing the MSE performance of frequency offset estimation, we adopt intelligent controllable LSPR parameter of ρ which is adjustable of the power ratio between the long training symbols and short training symbols. Based on the simulation results, it is found that proposed estimation scheme shows better MSE performance except for specific SNR region. For OFDM-based packet communication systems such as IEEE802.11a or IEEE802.11p, using the proposed scheme combining with SNR estimation scheme, we can achieve better MSE performance than conventional scheme in all SNR regions.

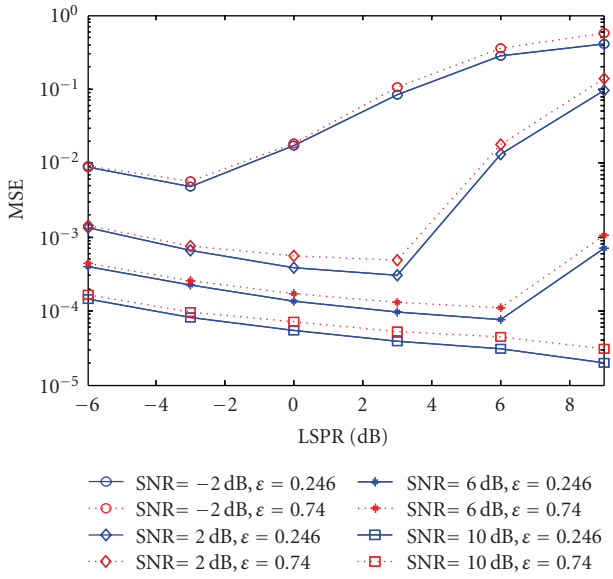

Figure 15: MSE performance of the proposed frequency offset estimation scheme according to LSPR parameter.

The proposed intelligent estimation schemes can be applied to the design and analysis for OFDM-based future generation intelligent communication network systems.

ACKNOWLEDGMENT

This research is supported by the ubiquitous Computing and Network (UCN) Project, the Ministry of Information and Communication (MIC) 21st Century Frontier R&D Program in Korea.

REFERENCES

[1] W. Y. Zou and Y. Wu, "COFDM: an overview," *IEEE Transactions on Broadcasting*, vol. 41, no. 1, pp. 1–8, 1995.
[2] http://www.ieee802.org.
[3] J. Heiskala and J. Terry, *OFDM Wireless LANs: A Theoretical and Practical Guide*, Sams, Indianapolis, Indiana, 2002.
[4] R. Prasad, *Universal Wireless Personal Communications*, Artech House, Boston, Mass, USA, 1998.
[5] T. Pollet, M. Van Bladel, and M. Moeneclaey, "BER sensitivity of OFDM systems to carrier frequency offset and Wiener phase noise," *IEEE Transactions on Communications*, vol. 43, no. 234, pp. 191–193, 1995.
[6] P. H. Moose, "A technique for orthogonal frequency division multiplexing frequency offset correction," *IEEE Transactions on Communications*, vol. 42, no. 10, pp. 2908–2914, 1994.
[7] T. M. Schmidl and D. C. Cox, "Robust frequency and timing synchronization for OFDM," *IEEE Transactions on Communications*, vol. 45, no. 12, pp. 1613–1621, 1997.
[8] S. Chang and E. J. Powers, "Efficient frequency-offset estimation in OFDM-based WLAN systems," *Electronics Letters*, vol. 39, no. 21, pp. 1554–1555, 2003.
[9] J. Li, G. Liu, and G. B. Giannakis, "Carrier frequency offset estimation for OFDM-based WLANs," *IEEE Signal Processing Letters*, vol. 8, no. 3, pp. 80–82, 2001.
[10] J. Medbo, "Radio wave propagation characteristics at 5 GHz with modeling suggestions for HIPERLAN/2," ETSI BRAN 3ERI074A, January 1998.
[11] W. C. Jakes Jr., *Microwave Mobile Communications*, John Wiley & Sons, New York, NY, USA, 1974.
[12] K. Pahlavan and A. H. Vesque, *Wireless Information Networks*, John Wiley & Sons, New York, NY, USA, 2nd edition, 2005.
[13] M. A. Ingram, G. Acosta, and L. Dong, "Wave channel model," IEEE802.11p Document, November 2006.
[14] IEEE Std 802.11a, "Wireless LAN medium access control (MAC) and physical layer (PHY) specifications: high-speed physical layer in the 5 GHz band," December 1999.
[15] IEEE 802.11p/D3.0, "Draft Amendment for Wireless Access in Vehicular Environments(WAVE)," July 2007.
[16] "ASTM E2213-03: Standard Specification for Telecommunications and Information Exchange Between Roadside and Vehicle Systems-5 GHz Band Dedicated Short Range Communications Medium Access Control and Physical Layer Specifications," 2003.